

# TIME-RESOLVED SIMULATION OF THE OPERATIONAL BEHAVIOR OF A TEST TURBINE FACILITY

*Fritz Neumayer*

Institute for Thermal Turbomachinery and Machine Dynamics-Graz University  
of Technology-Graz-Austria- neumayer@ttm.tu-graz.ac.at

## ABSTRACT

This paper describes the numerical simulation of a test turbine facility. Starting from the steady state solution the time dependent behavior of the coupled thermal and mechanical system was analyzed. These transient analyses focus mainly on shutdown strategies in the case of component failures but also on the simulation of load changes.

The steady state calculations were processed with IPSEpro, which is PC software for simulation of basically thermodynamic process. For the transient calculations the commercial static solver was replaced by a dynamic solver that can process the mixed system of differential and algebraic equations. One paragraph describes the implemented algorithm. The main equations describing the component models for the simulation are shown. Calculation results of an emergency shutdown case as well as of a load change example are compared to measured data.

## NOMENCLATURE

### Latin

$A$	[m <sup>2</sup> ]	area
$a$	[-]	coefficient
$c$	[m/s]	velocity (absolute)
$d$	[m]	diameter
$f, F$	[-]	function of
$g$	[-]	function of
$h$	[kJ/kg]	static enthalpy
$I$	[kgm <sup>2</sup> ]	moment of inertia
$m$	[kg]	mass
$\dot{m}$	[kg/s]	mass flow
$M$	[Nm]	torque
$n$	[rpm]	rotational speed

$p$	[bar]	pressure
$P$	[kW]	power
$r$	[-]	stage reaction
$s$	[kJ/kgK]	entropy
$t$	[s]	time
$T$	[K]	temperature
$u$	[m/s]	circumf. velocity
$U$	[kJ]	internal energy
$\dot{V}$	[m <sup>3</sup> /s]	volume flow
$w$	[m/s]	velocity (relative)
$X$	[-]	state vector

### Greek

$\alpha$	[°]	absolute flow angle
----------	-----	---------------------

$\delta$	[s]	time step	$l$	section 1 (downstream of nozzle)
$\Delta$		difference		
$\beta$	[°]	relative flow angle	$2$	section 2 (downstream of blades)
$\eta$	[-]	isentropic efficiency		
$\Pi$	[-]	pressure ratio	$d$	design
$\rho$	[kg/m <sup>3</sup> ]	mass density	$igv$	inlet guide vanes
$\zeta$	[-]	loss factor	$in$	inlet
$\Omega$	[1/s]	angular velocity	$out$	outlet
<b>Subscripts</b>			$R$	reservoir
*		critical	$s$	isentropic
$0$		section 0 (upstream of nozzle)	$u$	circumferential direction
			$\tau$	index of timestep

## INTRODUCTION

In November 1999 the turbine test facility at our institute was completed. This test stand is a cold flow transonic test turbine facility, which is a unique combination of a max. 2.5 MW axial test turbine and a directly coupled compressor that generates most of the compressed air needed to drive the turbine. To cover the losses additional air is provided by a separate, electrically driven compressor station. About 47 per cent of mass flow are fed by the compressor station and 53 per cent by the brake compressor. The compressor station consists of two turbo and two screw type compressors which may be operated in many different configurations (basically either in parallel or in series) in order to obtain different mass flows and pressure ratios.

The brake compressor which is equipped with variable inlet guide vanes is limited to a peak pressure of 4.5 bar.

A 600 kW suction blower driven by a helicopter turbine and decreasing the turbine exhaust pressure allows to increase the expansion ratio up to 5 (Erhard and Gehrler, [1]). This suction blower which can be seen in the upper left of Figure 1 may be operated if the turbine stages to be tested require high pressure ratios.

The flows of both compression devices (compressor station and brake compressor) unify in a mixer which is situated directly at the turbine inlet. The high pressure piping system together with the mixer form a cavity of about 14 m<sup>3</sup> storing energy in the form of pressurized air.

Each part of the flow path is equipped with pressure and temperature probes in order to measure the flow states as well as the mass flow. The turbine section allows access for conventional as well as optical measurement devices. Figure 1 shows the flow configuration of the test facility as it is currently operated.

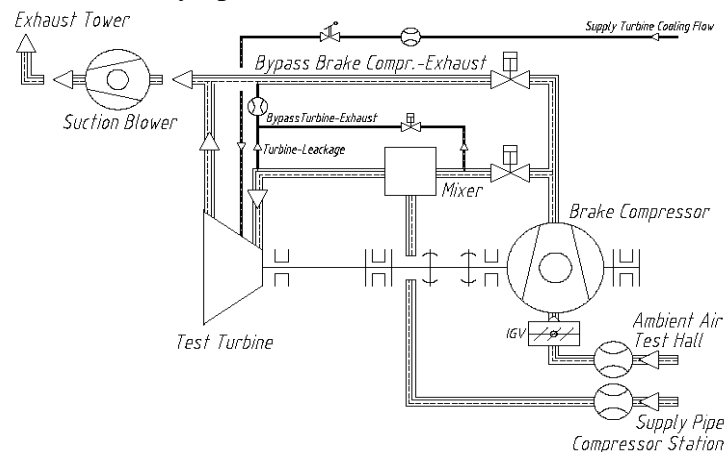


Figure 1 : Configuration of the test turbine facility

Basically three remotely controlled butterfly valves are used to perform startup, control and shutdown. Each of the valves is turned by two spring loaded pneumatic cylinders (see Figure 2). The valves are closed by pressurizing the pneumatic cylinders. If the pressurized air is discharged from the cylinders the large springs can open the flaps within 0,4 s. Figure 3 shows test turbine (at the left) and brake compressor (at the right) connected by the overflow pipe.

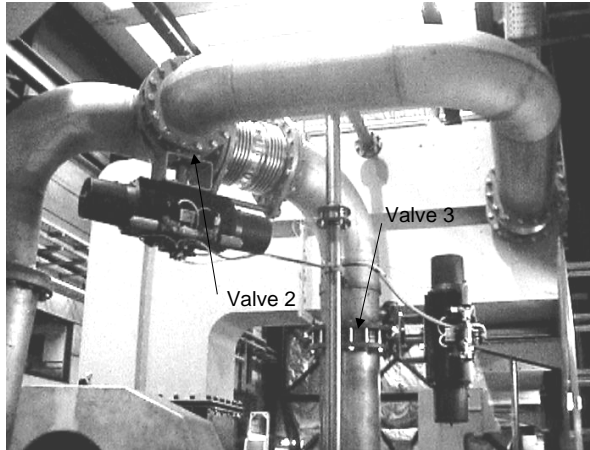


Figure 2 : Piping with butterfly valves

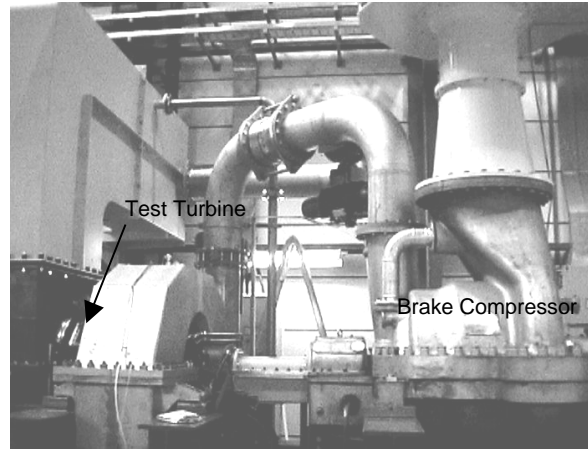


Figure 3 : Turbine and brake compressor

The dynamic calculations that will be shown were mainly motivated by investigations on the operational security of the facility to be built. During the design phase of the facility the question arose, in which time it were possible to stop the test turbine in the case of any failure and if it were possible to prevent the disintegration of the turbine rotor in the case of a failure of the coupling between the turbine and the brake compressor.

Besides that the control mechanisms of the test turbine should be simulated in advance.

Since the completion of the test stand a lot of test runs with two different turbine stages have been carried out so that the calculation results could be compared to measured data.

## COMPUTATIONAL TOOLS

The calculations shown were processed with IPSEpro, which is a package for simulation of basically thermodynamic process. The commercial version of this software includes a solver for static analysis (Perz [2]). The static process variables were evaluated using this solver. Starting from the static solution the dynamic response to time-dependent changes of parameters (i.e. valve opening angles, IGV angle) was investigated using a dynamic solver that is not included in the commercial version of the software yet.

### Implemented Algorithm of the Dynamic Solver

Gear [3] suggested a method, which does not require separating the differential and the algebraic equations of the mixed equation system. Given the representation of the system:

$$\mathbf{F}(\mathbf{X}_\tau, \dot{\mathbf{X}}_\tau) = \mathbf{0} \quad (1)$$

He replaced the derivative term by a difference approximation. The resulting set of algebraic equations should then be solved using Newton's method. If implicit Euler's method is used as the difference approximation, then the system of equations that must be solved at each step is:

$$\mathbf{F}(\mathbf{X}_\tau, \frac{\mathbf{X}_\tau - \mathbf{X}_{\tau-1}}{\delta_\tau}) = \mathbf{0} \quad (2)$$

The difference approximations most commonly used to represent the differential component in this expression are the backward differentiation formulas (BDFs) and some Runge Kutta methods.

Petzold [4] developed DASSL, an implementation of Gear's approach. DASSL uses polynomials to approximate the differential components. The algorithms used are an extension of the basic formulation given in Eq.(2). Instead of using the first order formula, DASSL approximates the derivatives using a k-th order polynomial, where k ranges from one to five. On every step it chooses the order k and step size  $\delta$  based on the behavior of the solution.

Using a k-th order polynomial the derivative  $\dot{\mathbf{X}}_\tau$  is expressed as a polynomial of  $\mathbf{X}_\tau$  at the last k integration steps:

$$\delta_\tau \dot{\mathbf{X}}_\tau = \sum_{j=1}^k a_j \mathbf{X}_{\tau-j} = a_0 \mathbf{X}_\tau + a_1 \mathbf{X}_{\tau-1} + \dots + a_k \mathbf{X}_{\tau-k} \quad (3)$$

$$\dot{\mathbf{X}}_\tau = c_j \mathbf{X}_\tau + \mathbf{C}_X \quad (4)$$

The substitution of Eq.(4) into Eq.(1) gives the system that has to be solved at each time step:

$$\mathbf{F}(c_j \mathbf{X}_\tau + \mathbf{C}_X, \mathbf{X}_\tau) = \mathbf{0} \quad (5)$$

This system of non-linear equations in  $\mathbf{X}_\tau$  is calculated using Newton's method.

## MODELLING

In the following the main components of the simulation model will be described. The component models are set up by the software user in a program called MDK (Model Development Kit). After that they are composed in another environment called PSE (Process Simulation Environment) which generates the input for the processor, performs the analysis and generates the output. One of the greatest advantages of the software package is the simple accessibility of physical property databases. The models generated in MDK are linked with connections.

The fluid connections transport the information on the state of the fluid as well as the magnitude of the mass flow from one model to the one that is connected. From these fluid connections the physical property databases are accessed. In this way multiple state variables may be calculated from at least two that are needed to define the state of the fluid. Another type of connection is the shaft connection which transports information on rotational speed and torque.

## COMPONENT MODELS

### Mass Storage Model

Basically the physical function of a mass storage for gases can be represented by the continuity and the energy equations ( Eq. (6) and Eq. (7)). (see Perl [5]).

Figure 4 shows the mass storage model with the basic variables.

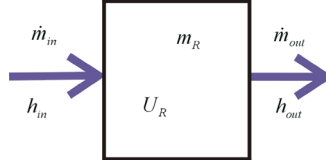


Figure 4 : Mass storage model

$$\dot{m}_{in} - \dot{m}_{out} = \frac{\partial m_R}{\partial t} \quad (6)$$

$$h_{in} \cdot \dot{m}_{in} - h_{out} \cdot \dot{m}_{out} = \frac{\partial U_R}{\partial t} \quad (7)$$

### Butterfly Valve Model

The mass flow through a valve depending on the flow area, the inlet- conditions and the downstream pressure is computed using Eqs.(8), (9), (10) and (11). It is supposed that the flow accelerates from zero speed isentropically to the point of the smallest flow area until the static pressure is equal to the backpressure. Afterwards the kinetic energy gets lost, entropy rises and the flow exits the valve with the same enthalpy as it had at the entry of the valve. If the backpressure is further decreased so that the pressure ratio is greater than the critical then the flow will only accelerate up to the speed of sound. In this case Eq.(8) which evaluates the speed at the point of the smallest flow area will be replaced by Eq.(9). The expansion through the valve is shown in Figure 6 for both the subcritical (left) and the supercritical case (right). From a given inlet pressure and inlet enthalpy and a given outlet pressure the mass flow will be iterated at each time step.

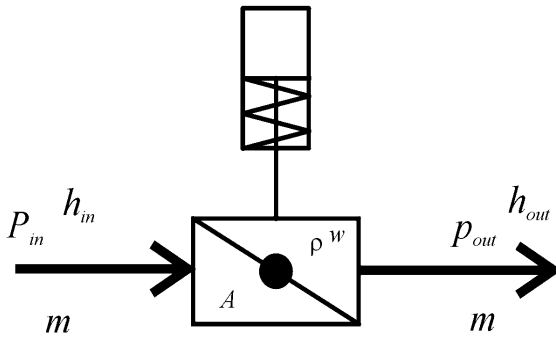


Figure 5 : Butterfly valve

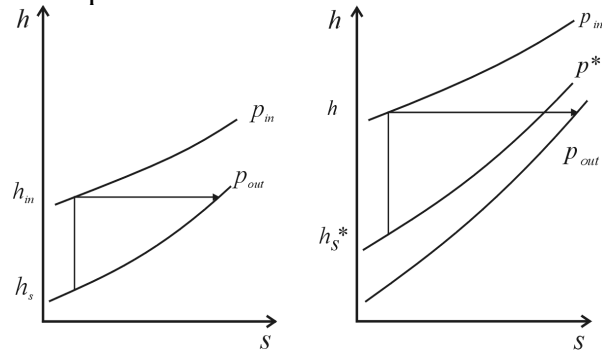


Figure 6 : Expansion through the valve

$$w = \sqrt{2 \cdot (h_{in} - h_s)} \quad (8)$$

$$w = \sqrt{2 \cdot (h_{in} - h_s^*)} \quad (9)$$

$$\dot{m} = \rho \cdot w \cdot A \quad (10)$$

$$A = f(t) \quad (11)$$

### Throttle Model

The formulation of the throttle is basically the same as that of the butterfly valve with the difference that the flow area of Eq.(11) is fixed.

### Compressor Model

A detailed compressor map that is included in the model describes the operational characteristics of the brake compressor.

The map used for is calculating the following function values:

- design speed volume flow calculated from pressure ratio depending on IGV angle (Eq.(12))
- design speed power consumption calculated from design speed volume flow depending on IGV angle (Eq.(13))

The following equations describe the mathematical formulation of the compressor:

$$\dot{V}_{in,d} = f(\Pi, \alpha_{igv}) \quad (12)$$

$$P_d = f(\Pi, \dot{V}_{in,d}) \quad (13)$$

$$P_d = \dot{m}_d \cdot \Delta h_d \quad (14)$$

$$\frac{\Delta h}{\Delta h_d} = \left( \frac{n}{n_d} \right)^2 \quad (15)$$

$$\frac{n}{n_d} = \frac{\dot{V}_{in}}{\dot{V}_{in,d}} \quad (16)$$

$$P = \dot{m} \cdot \Delta h \quad (17)$$

### Turbine Model

The formulation of the model representing the test turbine is based on a simple stage calculation in the midspan section. Mass flow at part load is calculated using the elliptic law (Eq.(18)). The following assumptions are made:

- Blading isentropic efficiency  $\eta_2$  depends on inlet angle  $\beta_1$  only, nozzle isentropic efficiency  $\eta_1$  is held constant.
- Angles  $\alpha_1$  and  $\beta_2$  are fixed. For the definition of angles  $\alpha$  and  $\beta$  refer to Figure 14 .

$$\frac{\dot{m}_{in}}{\dot{m}_{in,d}} = \sqrt{\frac{\frac{P_{in}^2 - P_{out}^2}{T_{in}}}{\frac{P_{in,d}^2 - P_{out,d}^2}{T_{in,d}}}} \quad (18)$$

$$\dot{V}_0 = c_0 \cdot A_0 \quad (19)$$

$$c_1 = \sqrt{\eta_1 \cdot (c_0^2 + 2 \cdot (1 - r_s) \cdot \Delta h_s)} \quad (20)$$

$$w_1 = \sqrt{c_1^2 + u_1^2 - 2c_1u_1 \cos(\alpha_1)} \quad (21)$$

$$h_0 + c_0^2 = h_1 + c_1^2 \quad (22)$$

$$\zeta = f(\beta_1 - \beta_{1,d}) \quad (23)$$

$$\eta_2 = \eta_{2,d} - \zeta \cdot \left( \frac{w_1}{c_1} \right)^2 \quad (24)$$

$$c_2 = \sqrt{w_2^2 + u_2^2 + 2 \cdot w_2 \cdot u_2 \cdot \cos(\beta_2)} \quad (25)$$

$$w_2 = \sqrt{\eta_2 \cdot (w_1^2 - u_1^2 + u_2^2 + 2 \cdot r_s \cdot \Delta h_s)} \quad (26)$$

$$h_2 = h_1 + \frac{w_1^2}{2} - \frac{w_2^2}{2} - \frac{u_1^2}{2} + \frac{u_2^2}{2} \quad (27)$$

$$P = \dot{m} \cdot \Delta(u \cdot c_u)_{1,2} \quad (28)$$

### Rotating Mass Model

The mass of compressor and turbine rotors is supposed to be concentrated at one position each (see Figure 8).

Torque balance will be calculated using Eq. (29) and Eq. (30) (see Figure 7)

$$M = M_{in} - M_{out} \tag{29}$$

$$M = I \cdot \frac{\partial \Omega}{\partial t} \tag{30}$$

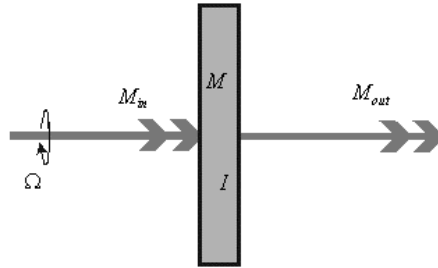


Figure 7 : Rotating mass model

### EMERGENCY SHUTDOWN SIMULATION

Figure 8 shows the simulation scheme for the calculation of the emergency shutdown. At the upper left of the figure a compressor symbol is drawn which represents the compressor station consisting of four compressors. Due to the angular momentum of the rotors the compressor station delivers air to the turbine for a certain amount of time after emergency shutdown being released. This occurs even if the bypass valve situated at the compressor station discharge (represented by “Valve 1” in Figure 8) starts to open immediately. In addition to that the big cavities of the piping system and the mixing chamber store about 14m<sup>3</sup> of pressurized air that is discharged after the release of emergency shutdown. The component model taking account for these cavities is marked with “Mass Storage” in Figure 8.

So the idea was to install a fast discharge valve (“Valve 2” in Figure 8) in order to release any air that would otherwise continue to drive the turbine after the shutdown of the compressor station. “Throttle 1” and “Throttle 2” take into account pressure losses that are in reality induced by the piping.

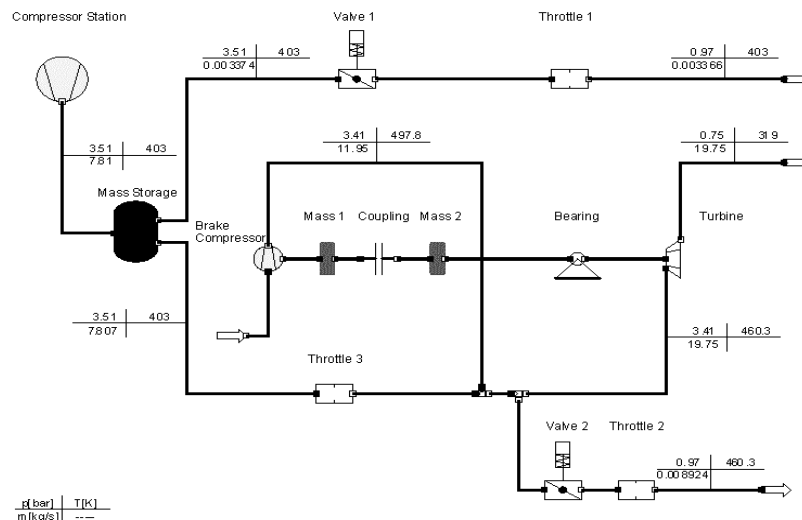


Figure 8 : Simulation scheme

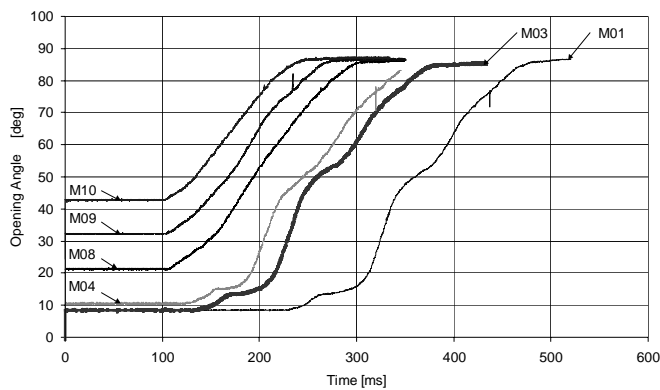


Figure 9 : Butterfly valve flap angles vs. time

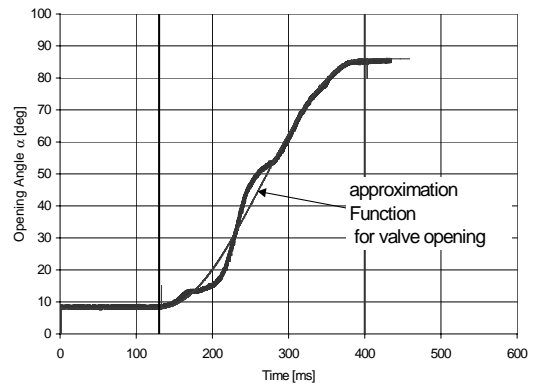


Figure 10 : Approximation function

Before the turbine facility was built the opening of a 350 mm spring loaded butterfly valve was measured and is shown in Figure 9.

The different curves result from variation of the initial pressure in the pneumatic cylinders and from different start angles. Curves “M04”, “M08”, “M09” and “M10” show the opening from not fully closed positions, “M01” shows the opening of the valve if the pneumatic actuator is filled with overpressure at the closed position. Curve “M03” shows the opening if the actuator pressure is reduced to 6 bar at the closed position. This pressure seems to be high enough to ensure correct sealing. For a time of 130 ms the pressurized air discharges from the spring- loaded cylinders of the actuator without turning the flap. After that time the flap opens within 270 ms. Figure 10 shows the harmonic function that was used for the approximation of the valve opening in the calculation (corresponding to the plot marked with “M03” in Figure 9).

## RESULTS

Results of the following calculations will be shown:

1. shutdown of the test facility from nominal speed without an additional release valve
2. shutdown of the test facility from nominal speed with an additional release valve
3. shutdown of the test facility after load release due to failure of the coupling to the brake compressor (at  $t = 0$ ) without an additional release valve
4. shutdown of the test facility after load release due to failure of the coupling to the brake compressor (at  $t = 0$ ) with an additional release valve (opens according to Figure 10)

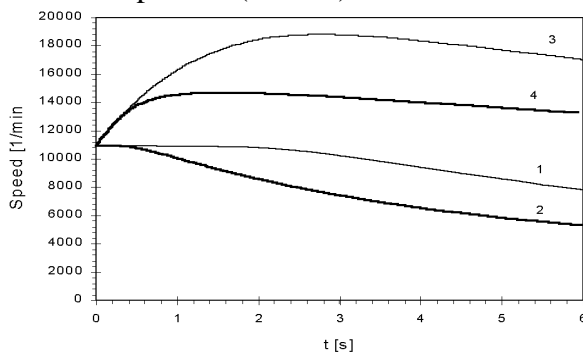


Figure 11 : Turbine speed versus time

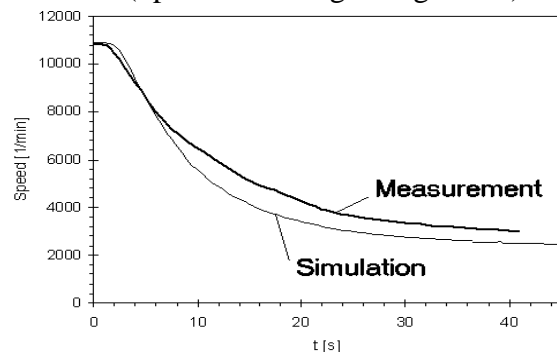


Figure 12 : Turbine speed measurement compared to calculation

Figure 11 shows turbine speed plotted vs. time for the four cases listed above (numbers corresponding). Notice that turbine speed would exceed 18000 rpm in the case that the coupling would fail and no additional discharge valve were installed. The rotor is expected to disintegrate at about 15000 rpm. Installing an additional release valve would limit the maximum speed to about 14700 rpm.

Figure 12 gives a comparison of the calculated speed to the measured for case No 1. The slight difference in deceleration between measurement and simulation lies in the big uncertainty of the loss coefficients of turbine and of bearing losses and/or the rough discretisation of the piping system.

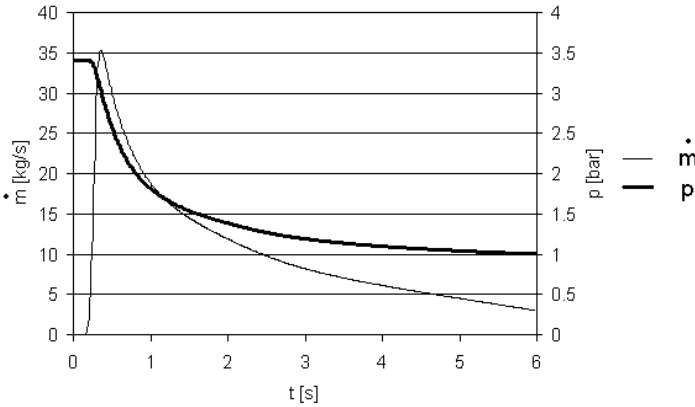


Figure 13: Pressure at inlet of and mass flow through additional discharge valve (“Valve 1”) for Case No.2

Figure 13 shows pressure at inlet of and mass flow through the additional discharge valve (“Valve 1” in Figure 8) for case No.2. Notice that after 0.13 s air starts to flow through the opening valve. After 0.38 s the mass flow reaches its maximum.

A look at the velocity triangles in Figure 14 at different times after the coupling failure (case No. 3) shows that the deviation of the flow in the rotating blades will decrease reducing the stage work very quickly. After about 3 seconds the turbine work will be negative which means that the turbine will work as a brake.

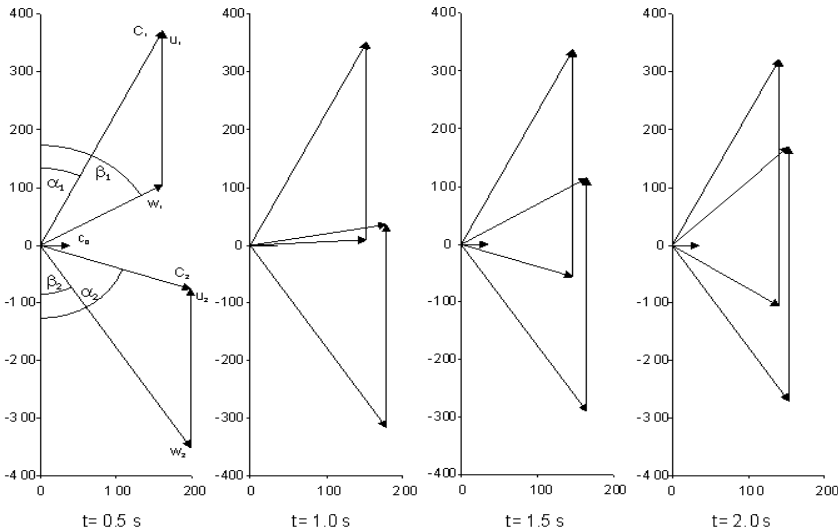


Figure 14 : Calculated velocity triangles at different times

## RESPONSE TO IGV ADJUSTMENT

The primary control mechanism of test turbine speed is the IGV angle adjustment of the brake compressor. In order to get information on how the turbine responds to quick closing of the IGVs the following simulation was done: From a stable operation condition at 9825 rpm (IGVs at neutral position) the IGVs were closed to the 20° position with maximum actuator speed (about 1° /s). The beginning of this adjustment is at  $t = 10$  s in the plot of Figure 15 . After the adjustment the calculation showed some oscillation before stabilizing at 10580 rpm. The response to such an adjustment was measured and is compared to the simulation in Figure 15 An interesting result is that the real system damps the oscillations better than the simulation model. This may be due to the fact that in the simulation the air mass is stored in one point of the system while in reality mass is stored in the long piping system. The pressure propagation through the piping is responsible for time delays and losses that are not covered by the simulation model. This might be responsible for the difference in oscillation frequency and damping. A finer discretisation and taking account for the shock propagation through the piping would possibly give more accurate results. The level at which the speed stabilizes after the igv adjustment is slightly higher than the calculation predicted. This may come from inaccuracies in the compressor mapping as well as from the very simple modeling of the flow through the turbine.

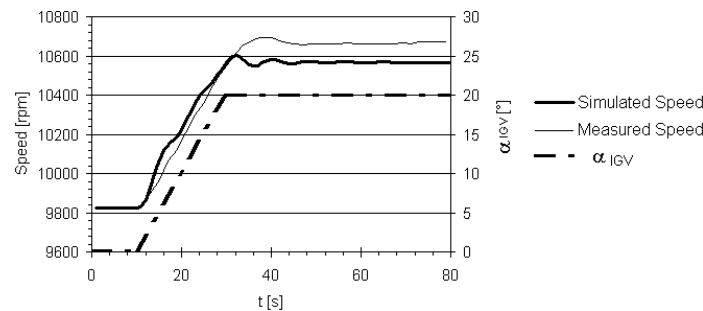


Figure 15 : Response to IGV adjustment

## CONCLUSIONS

It has been demonstrated that a simulation program package for steady state thermodynamic analysis was modified in order to allow dynamic calculations. The algorithm of the dynamic solver that was inserted was described as well as the basic equations. The application of the solver described was shown with calculating the emergency shutdown and a load change example of the turbine test facility at Graz University of Technology. In future applications the discretisation of the components should go more into details in order to get more accurate results.

The software with the dynamic solver may be available for the public soon, making it easy even for users who do not have to deal with conventional programming to create their own component models and processes and simulate thermo- mechanical systems like the one that has been presented.

## ACKNOWLEDGMENTS

The author gratefully acknowledges the support of SimTech Simulation Technology for integrating the dynamic solver. He thanks the Austrian Science Foundation (FWF) for supporting this work (Project S6801 “Efficiency improvement by flow optimization”) as well as the support of the European Commission (Project DITTUS “Development of Industrial Transonic Turbine Stages”).

## REFERENCES

---

- [1] Erhard, J., Gehrler, A. (2000). *Design and Construction of a Transonic Test-Turbine Facility*. ASME Paper 2000-GT-480
- [2] Perz, E. (1991). *A Computer Method for Thermal Power Cycle Calculation*. Journal of Engineering for Gas Turbines and Power, Vol.113, April 1991, 184-189.
- [3] Gear, C. W. (1971). *The simultaneous numerical solution of differential-algebraic equations*. IEEE Trans Circuit Theory, CT-18, 89-95
- [4] Petzold, L. (1982). *Differential/Algebraic equations are not ODE's*. SIAM J. Sci. Stat. Comput., 3, 367-384
- [5] Perl, T. (1990). *Beitrag zur Simulation von Kraftwerksprozessen –Schnellschlußfall*. Diploma Thesis, Institute for Thermal Turbomachinery and Machinery Dynamics, Graz University of Technology